JOURNAL OF MATERIALS SCIENCE 14 (1979) 882–890

The fracture and fatigue of sintered diamond compact

K. J. DUNN, M. LEE
General Electric Company, Corporate Research and Development, Schenectady, New York 12301, USA.

The fracture stress of the sintered diamond compact is reduced under cyclic loading. The measurements were made using a dynamic test machine, with a diamond compact cutter impacting onto cemented tungsten carbide. The fracture mode under the present experimental conditions is brittle shear fracture. Crack growth is believed to be promoted by a relatively small tensile stress component at the tip of the crack due to the very large applied shear stresses. A possible failure mechanism is proposed based on examination of SEM micrographs of the damaged area. The results obtained in the present test indicate that the asymptotic value of the failure load corresponding to an infinite number of cycles is far above the reported value of force for cutting rocks under similar geometric conditions.

1. Introduction

Sintered, high-density polycrystalline diamond compacts have shown excellent performance characteristics in operations such as machining, dressing, wire drawing and rock drilling. Some of these uses involve situations where the sintered diamond compact is subject to cyclic stress. Particularly in rock drilling, where the rock is fragmented chip by chip in a brittle manner, the drill bit actually experiences complex cyclic impact loading. Thus, in designing these parts it is important to know the impact and fatigue behaviour of the bit material.

Various laboratories have reported fatigue phenomena of brittle materials such as Al_2O_3 ceramics and diamond, i.e. a reduction in fracture stress for situations in which the stress is cyclic. Huffine and Berger [1] reported a study on impact fatigue of polycrystalline alumina. They found that the strength under cyclic impact loading was reduced to 60% of the static strength. They also discussed the effect of the presence of a second phase. Bowden and Tabor [2] described briefly a study by Hancox on the effect of repeated impacts of a tungsten-carbide ball on a single crystal diamond surface at room temperature. Ring cracks were produced at a stress level well below the static failure stress. Recently, Bell *et al.* [3] also observed that repeated indentations of a single crystal diamond surface by a spherical diamond indenter, using 75% of the critical load required to produce a fully developed ring crack, would cause progressive build-up of surface damage and the eventual appearance of short cracks lying along cleavage planes. Our present work on sintered diamond compacts also indicates the existence of this fatigue-type failure.

The primary purpose of this work was to investigate the ultimate mechanical strength of sintered diamond compacts under dynamic cyclic loading both at room temperature and at a higher temperature near 300° C, with an angle of impact similar to that of a rock drilling system. Initially, a Jackfork Sandstone surface was chosen to be impacted by the sintered diamond compact cutter, in order to simulate closely the condition of a rock drilling system. However, the diamond compact was so strong that it made a large indentation on the rock surface at the relatively low load of 200 to 300 lb* and with increasing load, it merely penetrated into the rock without increasing the local stress. After a total number of 10^5

*1 lb = 4.5359×10^{-1} kg.

cycles, no damage was observed on the sintered diamond compact. It was impossible to find the ultimate strength of the compact by using the strongest rock available to us. Therefore, cemented tungsten carbide (13% Co) was chosen to be the surface impacted by the diamond compact cutter in subsequent tests. With this combination, the failure of the compact at the edge was finally observed at fairly high loading. The results show that the fracture stress is reduced as the total number of cycles is increased, suggesting a fatigue-type failure. Since diamond is an extremely brittle substance, fatigue effects, if they occur, must arise in a different way from the usual process in metals which involves plastic deformation and work-hardening. Possibly some irreversible processes are occurring in the specimen which involve opening and incomplete closure of sub-critical cracks followed by gradual growth of these small cracks due to cyclic stress.

It is to be noted here that the compact cutter in the present test was subjected to much more severe local stress than the reported stress on the cutting edge of compacts in a rock cutting system [4].

In the following section, the experimental method will be described and the results discussed. A possible failure mechanism is proposed based on an approximate stress analysis of the specimen and on examination of SEM micrographs of the damaged area.

2. Experiments and results

The test specimens were sintered polycrystalline diamond compacts. These are round discs (13.3 mm diameter) of polycrystalline diamond bonded to a cemented tungsten carbide substrate. The overall thickness of a blank is 3.3 mm including a minimum diamond layer thickness of 0.5 mm. The blanks were first bonded to carbide slugs and then pressed into pockets of steel holders. The interference between the diameter of a carbide slug and the pocket diameter in a steel holder was about 0.025 mm. This simple holder (compact/slug system) was positioned into a jig fixture as shown in Fig. 1. The whole assembly was then attached to a dynamic test machine as shown schematically in Fig. 2. The machine is manufactured by the Lawrence Division of CGS Scientific Corporation (Model 109). It is a completely integrated Electro-Hydraulic Servo-Control System consisting of an electronic console, a load or reaction frame and a hydraulic pumping station. One can control the applied force in either tension or compression in the form of a sinusoidal, sawtooth or square-wave function. In the present study, a sinusoidal

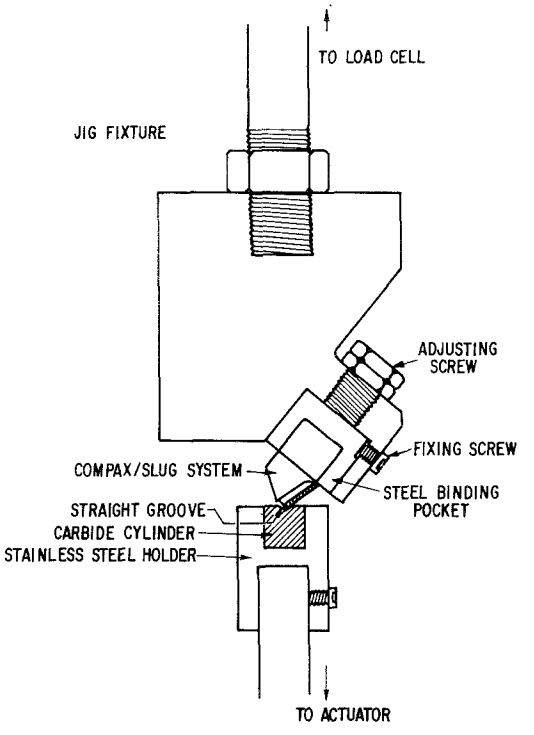

Figure 1 Schematic view of the specimen jig fixture for incorporation into a dynamic test machine.

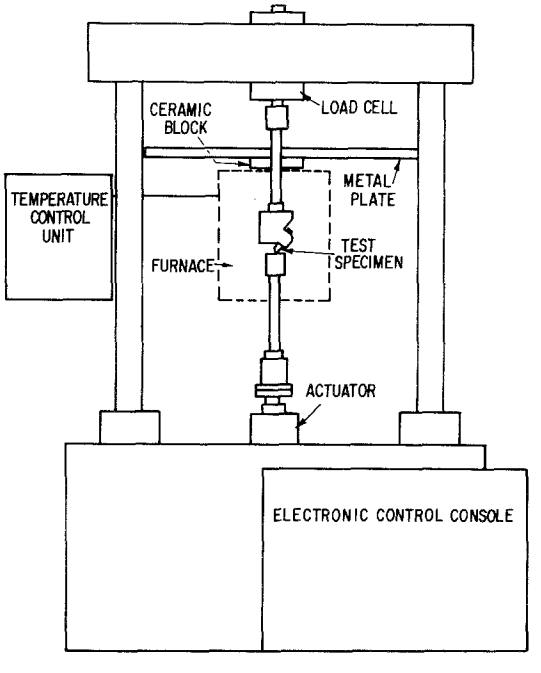

Figure 2 Schematic diagram of the dynamic test machine.

form was chosen and only the compression mode was used.

From their rock cutting experiments, Hibbs and Flom [4] reported that for a certain type of rock, the diamond compact experienced a resultant force which varied in both magnitude and direction depending upon the cutting speed, depth of cut, and rake angle chosen. They found that the diamond compact cutter experienced the least resultant force at a negative rake angle between 10° and 20°. Based on this information, the present experiments were designed in such a way that the diamond compact test specimen has a negative rake angle of 15°, a resultant force angle of 40° and a simulated depth of cut of 1.27 mm. The schematic details are shown in Fig. 3. During the test, the dynamic test machine provided a cyclic force, partially simulating the condition that a diamond compact would experience in real rock drilling. Hence, the direction of the resultant force which the rock (in our experiment, it is tungsten carbide cylinder) exerted on the diamond compact cutter was aligned along the direction of the stroke of the actuator.

In order to ensure good contact with a measurable area while the specimen was cyclically loaded, a tungsten carbide cylinder with a straight groove across the flat surface on one end was fitted into a stainless steel holder. One side (surface A) of the groove had an angle of 35° with respect to the flat cylindrical end and was designed to make intimate contact with the diamond compact surface. The other side (surface B) of the groove had an angle of 40° with respect to the flat end and made point contact with the diamond compact edge under an initial low load. As the load was increased, surfaces A and B were deformed plastically. By measuring the contact area, the maximum normal stresses σ_x and σ_y could be estimated.

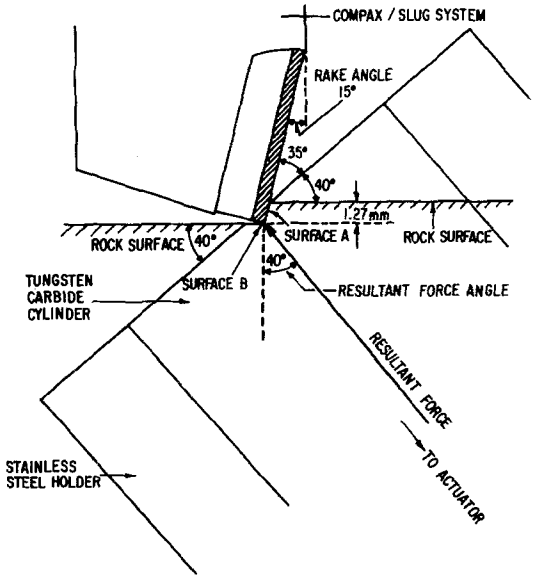

Figure 3 The test specimen in contact with the carbide cylinder.

For a preset functional load, the actuator received the command signal and moved upward until the carbide cylinder hit the specimen. The force was continuously increased according to the prescribed functional form and was sensed by the load cell at the top of the machine. When the load reached a maximum, the actuator moved downward and the cycle repeated according to the preset frequency. The cycling force varied between zero and a preset maximum load in a sinusoidal manner and was generally of negative sign, i.e. in a compression mode. For frequencies below 10 Hz, impact conditions could be obtained by adjusting the mean level of the signal wave such that at the end of the unloading cycle, the command signal was in a tension mode. At that stage the carbide cylinder would leave the specimen momentarily. As soon as the signal became negative, the carbide cylinder moved upward and hit the specimen again. However, for frequencies higher than 10 Hz, the actuator could not respond fast enough to provide impact. The carbide cylinder would then always be in contact with the specimen with a minimum force of about 10 to 20 lb.

Although we had an impact situation for low frequencies, the experiment was not designed to measure such parameters as impact velocity and energy transfer.

For our present tests, each specimen was subjected to a force between zero and the maximum load for a given number of cycles. The specimen was then taken out and examined under a microscope. If there was no visible damage, the specimen was put back and stressed for an additional number of cycles. This process was repeated until failure was observed. The results are shown in Fig. 4. A datum point was recorded for the total number of cycles at which a specimen was found to have failed (i.e. edge fractured). The error bar on the plot was extended back to the total number of cycles where the specimen was last examined and found to have no visible damage. Clearly, failure occurred between these

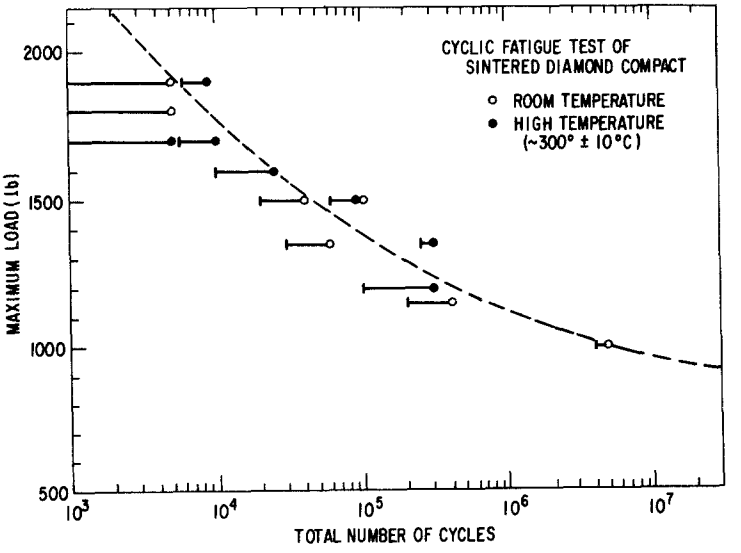

Figure 4 Maximum force in cyclic loading versus the total number of cycles that lead to failure of the sintered diamond compact.

two numbers of cycles. The failure was defined as any visible crack slit or chipped-off edge. Of the 14 specimens tested, only one had a crack slit on the edge without complete failure. The remaining specimens chipped in very similar manner. For the high temperature tests, the specimen was preloaded to approximately 60 lb. The temperature was increased to 300 ± 10° C and held there until thermal equilibrium was reached. The specimen was then cycled in the same way as in the room temperature test. The results are also shown in Fig. 4. These show a similar relationship of load versus total cycles to failure as an S–N curve for ordinary fatigue. For data below 10^5 cycles, the cycling frequencies were mostly 5 or 10 Hz. For data beyond 10^5 cycles, frequencies as high as 30 Hz were used. Within the limits of these data, no effects of frequency on failure were observed in our present experiments. Also, there was no appreciable difference between the high temperature results at 300 ± 10° C and those at room temperature.

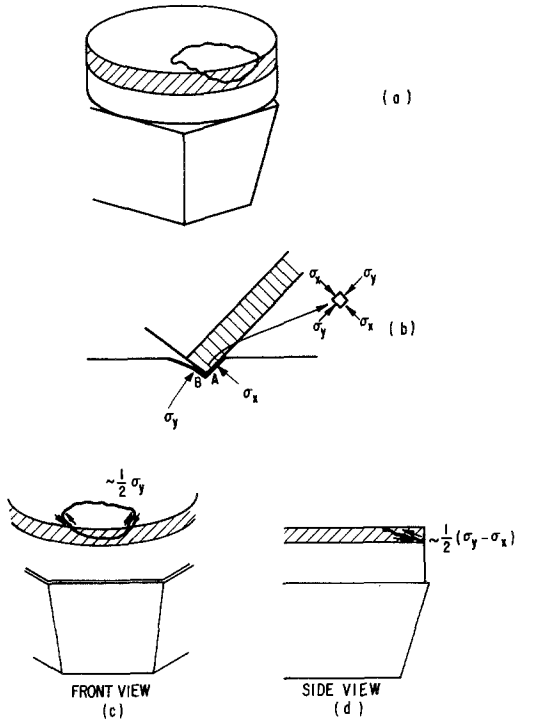

Figure 5 General fracture pattern of the test specimen.

3. Analysis and discussion

The general shape of the fractured edge of most of the broken diamond compacts has a pattern as shown in Fig. 5a. The direction of the crack is generally the same as that of the maximum shear stress, suggesting that failure occurred by shear. When the diamond compact was in contact with the groove on the carbide cylinder, there were two normal stresses, σ_x, σ_y acting on the edge of the specimen as shown in Fig. 5b. The stress distribution within the edge could be crudely expressed as:

$$\begin{pmatrix} \sigma_x & 0 & 0 \\ 0 & \sigma_y & 0 \\ 0 & 0 & 0 \end{pmatrix}$$

To find the maximum shear stress in the system, one can rotate the co-ordinates about z-axis or x-axis by an able θ. The stress tensor in the new

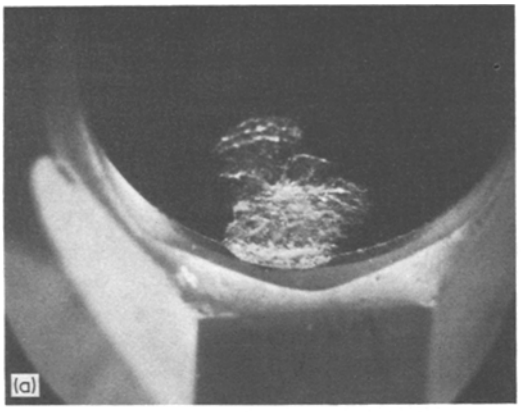

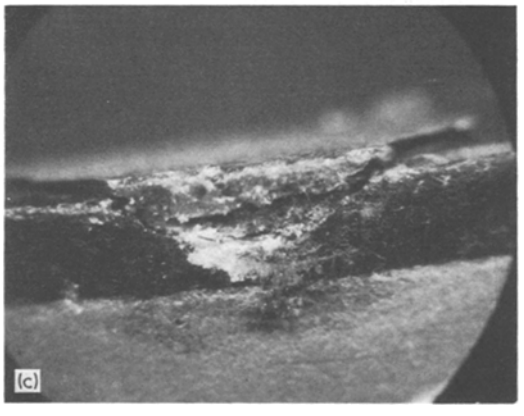

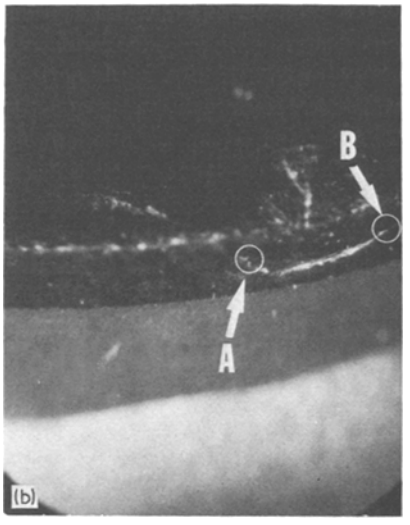

Figure 6 Optical photomicrographs showing the general fracture pattern of test specimens.

co-ordinates can be expressed respectively as:

$$\begin{pmatrix} \sigma_x \cos^2\theta + \sigma_y \sin^2\theta & 1/2(\sigma_y - \sigma_x)\sin 2\theta & 0 \\ 1/2(\sigma_y - \sigma_x)\sin 2\theta & \sigma_x \sin^2\theta + \sigma_y \cos^2\theta & 0 \\ 0 & 0 & 0 \end{pmatrix}$$

or

$$\begin{pmatrix} \sigma_x & 0 & 0 \\ 0 & \sigma_y \cos^2\theta & 1/2\sigma_y \sin 2\theta \\ 0 & 1/2\sigma_y \sin 2\theta & \sigma_y \sin^2\theta \end{pmatrix}.$$

The maximum shear stress, $\sim 1/2\sigma_y$, occurred at 45° with respect to the compact edge as shown in Fig. 5c. Another shear stress, $\sim 1/2(\sigma_y - \sigma_x)$, occurred at 45° with respect to the compact surface as shown in Fig. 5d. Although the stress distribution within the edge of the specimen was predominantly compressive so the propagation of any micro-cracks within the specimen or of cracks from surface flaws would be suppressed, it was possible for cracks to form and propagate under shear stress aided by a small tensile stress near the shear plane. These shear stress would promote crack growth in a step by step brittle manner until a critical condition was reached at which rapid failure would occur.

Fig. 6a to c shows typical crack patterns where the crack can be seen running along the direction of a maximum shear stress.

Specimen 1 failed for a 0 to 1500 lb cycle at a total of 10^5 cycles. The contact area was measured, and the normal stresses σ_x and σ_y were estimated to be:

$$\sigma_x \sim 90\,000 \text{ psi}^*$$

$$\sigma_y \sim 700\,000 \text{ psi}.$$

The corresponding maximum shear stresses were:

$$1/2\sigma_y \sim 350\,000 \text{ psi}$$

$$1/2(\sigma_y - \sigma_x) \sim 305\,000 \text{ psi}.$$

It should be noted that the value calculated here is only qualitative since σ_y was not really uniform on the contact area. Gigl [5] measured the transverse rupture strength (TRS) of the sintered diamond compact in a three-point bending test as 120 000 psi. However, no attempt is made here to correlate our measurement with his because of the complexity of the real stress distribution near the cracks of the specimen and the dynamic nature in the present experiment.

Another factor which could be hypothesized to contribute to failure arises from the shock wave

*10^3 psi = 6.89 N mm^{-2}.

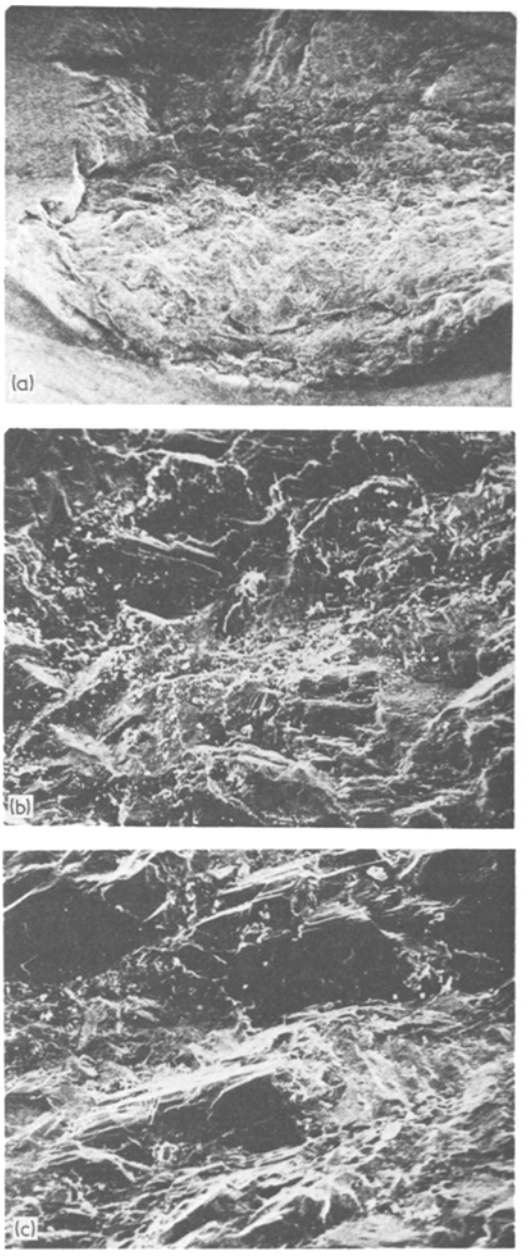

Figure 7(a) SEM showing the overall view of the crack surface of specimen 8 (× 18). (b) SEM showing the area of the crack surface close to the edge for specimen 8 (× 240). (c) SEM showing the area in the back of the crack surface for specimen 8 (× 240).

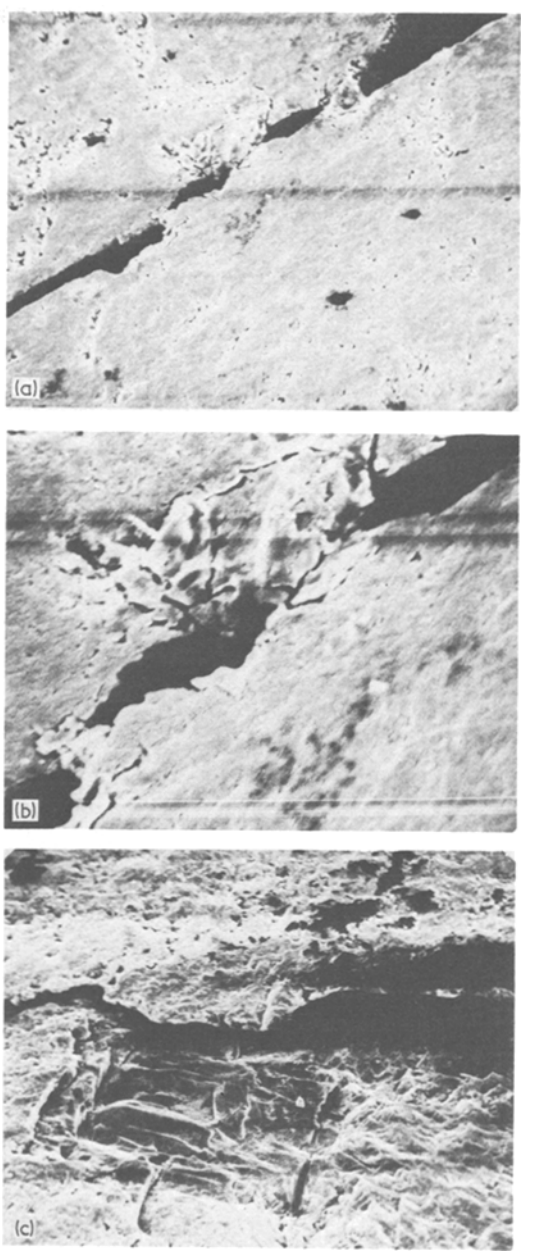

Figure 8(a) SEM showing the crack slit of area B in Fig. 6b (× 420). (b) Magnified view of (a) (× 1200). (c) SEM showing the crack slit of area A in Fig. 6b (× 420).

due to impact loading. When a shock wave is reflected from the back of a specimen, a tensile pulse is generated and, if sufficiently great, this can promote crack growth. Since in the present experiments the specimen was not hit by a high velocity impact and was in contact with the carbide cylinder for 90% of the cycle duration at relatively low frequency, it is believed that this factor was negligible in the failure mechanism.

In order to investigate the fracture mechanism further, several SEMs were taken for specimens 1, 3 and 8. The crack surface close to the edge has an irregular shape with many pulverized diamond particles present, while the rear area of the crack surface exhibits a more clearly defined pattern with many large cleavage planes. Fig. 7a shows

the overall view of the crack surface of specimen 8. Fig. 7b was taken at an area close to the edge, while Fig. 7c was taken at an area in the back. One can clearly see the difference between the two surfaces. Specimen 3 was the only one that had a crack slit without complete fracture of the edge. Micrographs were taken of the crack slit at the cylindrical surface of the diamond compact. Fig. 6b shows the overall appearance of the crack. Fig. 8a shows one end of the crack slit, inclined 45° to the top surface of the diamond compact, and Fig. 8c shows the opposite end of the same crack, also with a 45° inclination to the top surface. It can be seen that the crack slit is rather large. However, the top corner of the cracked edge (shown in Fig. 6b) is still strongly bonded to the compact and it could not be broken apart with several severe blows with a hammer. Specimen 3 probably represents the first stage of failure for a specimen such as no. 8. If it had been cycled further, it could have produced a chipped-off edge like specimen 8. Close inspection shows that Fig. 8a includes many diamond grains on both sides of the crack slit. Individual diamond grains in compacts are distinguishable by small pit marks created at grain boundaries along the surface grinding process. These pit marks are formed by preferential removal of trapped metal inclusions located at the grain boundaries.

A crack could be initiated from any one of the following possible sources: surface flaws from grinding, inherent microscale flaws inside the diamond grains, and fine defects at internal grain boundaries. However, these defects are generally either very small, e.g. most of the internal flaws, or they have large effective crack tip radii characteristic of grinding pit marks. Therefore, a relatively high stress would be required to initiate macroscopic cracks from these defects. The materials exhibit high bend rupture strengths. Under cyclic loading conditions such as in our tests, each individual stroke was not sufficient to initiate massive fracture but rather would increase the number and size of the flaws. Eventually, cracks would be initiated from these flaws and would grow step by step in a brittle manner. Between steps, a crack would change direction due to several reasons. It would change its direction at the grain boundaries because of the change of the preferred cleavage direction from one grain to another. Alternatively, the crack could stop or by-pass the metal inclusion at the grain boundaries. Also, a crack could alter its direction on encountering twin boundaries in the diamond grains, these twin bands having been generated during the compact synthesis. One clear example is shown in Fig. 9a. This was a fracture surface produced by a single stroke obtained by making

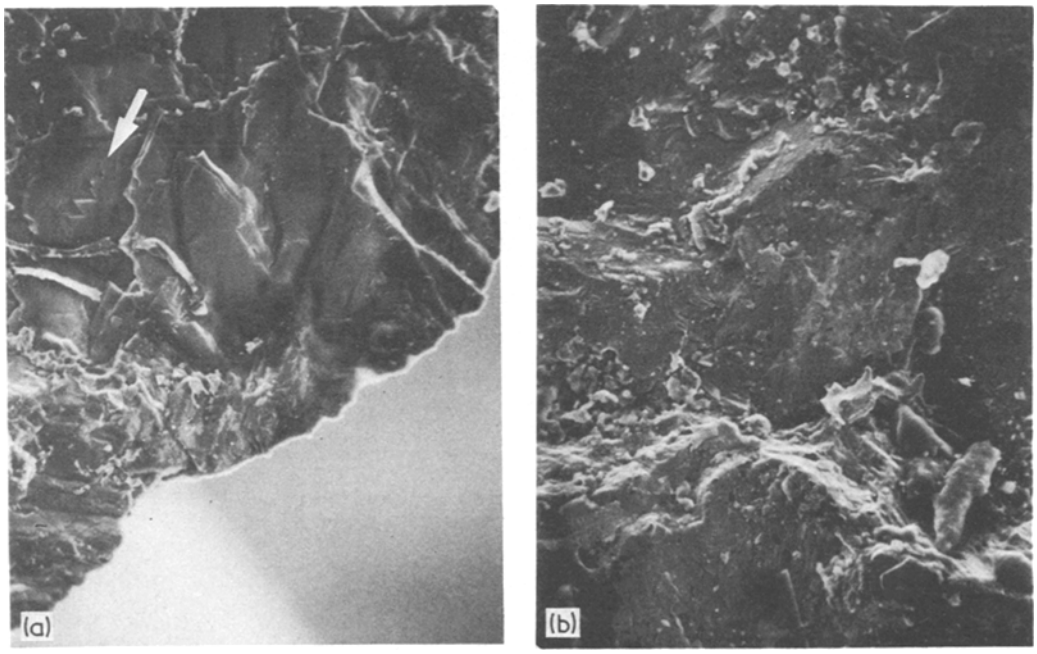

Figure 9(a) SEM showing the crack surface produced by a single fracture. The zig-zag pattern is shown by an arrow (× 525). (b) SEM showing the area of the crack surface close to the edge for specimen 1 (× 525).

a cut half way into the disc from the carbide side of the diamond compact and then snapping it. A sharp zig-zag pattern (shown by an arrow) in the middle of a cleavage plane clearly shows the effect of the deformation twin bands on the formation of this fractured surface. We would expect similar features in the cracks from a cyclic fatigue test. However, this clean, flat, fracture plane and the zig-zag pattern were completely obliterated by the mechanism which we shall now discuss.

The diamond layer of the compact is generally under residual compressive stress due to the nature of its composite structure and the process condition to which it has been subjected. Hence, in these tests when a crack developed parallel or nearly parallel to the top surface of the compact, the top side of the crack would undergo some elastic relief. As a result, when the two mating surfaces of the crack were pushed together by subsequent stress, they would not match exactly. Some of the high points of the irregular fracture surfaces made the first contact, and the local stresses at these points were exceedingly high. This would cause microchipping of the fracture surfaces. Unlike the asperity contacts of two metal surfaces which deform plastically, the diamond asperity contacts underwent brittle fracture leaving widely scattered diamond debris around the crack surface. These small diamond particles would again cause further microchipping of the crack surface, making the crack slit larger and larger. After the initial period of this microchipping process, the contact between the cracked surfaces reached a semi-stable condition at which the contact area became as large as a grain. At this stage, the local stress was not large enough to fracture the entire grain, but it would cause the grain to undergo a mini-scale fatigue failure process, until the whole grain has broken away leaving an intergranular fracture surface. This phenomenon is depicted in Fig. 8a and b, where one can see that a grain at the contact point was shaken loose and ready to be ejected. This could explain the appearance of the front part of the crack surface shown in Fig. 7a, the magnified view of the same area shown in Fig. 7b for specimen 8, the large crack slit shown in Fig. 8b for specimen 3, and the crack surface close to the edge for specimen 1 shown in Fig. 9b. All of these figures indicate an initially clean fracture surface obscured by the microchipping process, leaving a surface which is a combination of irregular cleavage patterns and an intergranular fracture surface with much small diamond debris present. Fig. 9b shows quite clearly the intergranular fracture pattern on some parts of the crack surface.

As the crack continued to develop and grow, at one point the critical condition would be reached, such that the local stress distribution, crack tip radius and crack direction would be favourable for spontaneous crack growth. At this point, massive fracture would occur and the remaining part would fail in a rapid manner. The fracture surface of this final stage of failure should be mostly transgranular in type with many large cleavage planes. This explains the appearance of the fractured surface shown in Fig. 7c. Fig. 9a, showing the crack surface obtained by a single stroke, exhibits more vividly the transgranular-type pattern.

It is not entirely clear exactly how the crack was initiated. Also, the role and the effect of the presence of the metal phase on the fracture mechanism are not fully understood.

In a real rock drilling system, the stress distribution is more complicated than in the present experiment. The relatively high speed rock particles may also provide a local shock impact effect.

From the experiments of Hibbs and Flom [4], we know that the resultant force experienced by the compact cutter in a rock cutting system at a negative rake angle of 15° and a depth of cut of 1.27 mm is about 70 to 120 lb depending on the cutting speed. This figure is far below our asymptotic value of failure load, i.e. approximately 800 lb corresponding to infinite number of cyles as shown in Fig. 4. This fact suggests a mechanical fatigue effect is not expected to be important in the idealized rock drilling system, i.e. in the absence of other potential factors such as high local shock impact.

4. Conclusions

(1) The fracture stress of a diamond compact is reduced under cyclic loading.

(2) The fracture of a diamond compact in the present experiments is a shear mode brittle fracture. Crack growth requires very large shear stresses because of the high strength of the diamond crystallites and the strong bonds present between diamond grains in these sintered compacts. Crack propagation is believed to be promoted by a relatively small tensile stress com-

ponent at the tip of the crack due to the large applied shear forces.

(3) SEM observations show a more irregular pattern for the crack surface close to the edge, and a more clean transgranular type of fracture pattern at the back of the crack surface.

(4) The conditions for a rock drilling system in practice are not the same as in the present experiment in that the former may involve more shock impact loading and other factors not considered in this study. However, it is noted that the failure load corresponding to infinite number of cycles is far above the reported values of force for cutting rocks under similar geometric conditions.

Acknowledgement

The authors wish to thank Dr D. G. Flom for critically reviewing the manuscript, and L. E. Hibbs for many helpful discussions. The support by the United States Department of Energy under contract No. EX-76-C-01-2360 is also acknowledged.

References

1. C. L. HUFFINE and C. M. BERGER, *Amer. Ceram. Soc. Bull.* **56** (1977) 201.
2. F. P. BOWDEN and D. TABOR, "The Friction and Lubrication of Solids", Part II (Oxford University Press, 1964) p. 163.
3. J. G. BELL, M. E. C. STUIVINGA, A. G. THORNTON and J. WILKS, *J. Phys. D.* **10** (1977) 1379.
4. L. E. HIBBS, Jr and D. G. FLOM, Energy Technology Conference, Houston, (September, 1977).
5. P. D. GIGL, Sixth AIRAPT International High Pressure Conference, Boulder, Colorado (July, 1977).

Received 12 May and accepted 29 August 1978.